

## Effect of Loading Protocols on Premature Shear Failure of Reinforced Concrete Bridge Piers with Termination of Main Reinforcements

Tomohiro SASAKI\*, Kazuhiko KAWASHIMA\*\*, Gakuho WATANABE\*\*\*, Seiji NAGATA\*\*\*\*, Kungsanant THARIN\*\*\*\*\*,  
Hiromichi UKON\*\*\*\*\*, Koichi KAJIWARA\*\*\*\*\*

\* Graduate Student, Dept. of Civil Eng., Tokyo Institute of Technology, 2-12-1, O-okayama, Meguro, Tokyo 152-8552

\*\* Dr. of Eng., Professor, Dept. of Civil Eng., Tokyo Institute of Technology, 2-12-1, O-okayama, Meguro, Tokyo 152-8552

\*\*\* Dr. of Eng., Assistant Professor, Dept. of Civil Eng., Tokyo Institute of Technology, 2-12-1, O-okayama, Meguro, Tokyo 152-8552

\*\*\*\* Dr. of Eng., Postdoctoral Researcher, Dept. of Civil Eng., Tokyo Institute of Technology, 2-12-1, O-okayama, Meguro, Tokyo 152-8552

\*\*\*\*\* Graduate Student, Dept. of Civil Eng., Chulalongkorn University, Bangkok, Thailand

\*\*\*\*\* Researcher, National Institute for Earth Science and Disaster Prevention, 1501-21, Mitsuta, Nishikameya, Shijimi, Miki, Hyogo,  
673-0515

\*\*\*\*\* Dr. of Eng., Researcher, National Institute for Earth Science and Disaster Prevention, 1501-21, Mitsuta, Nishikameya, Shijimi, Miki,  
Hyogo, 673-0515

A number of bridges suffered extensive damage during the 1995 Kobe, Japan earthquake due to premature shear failure resulted from termination of longitudinal reinforcements with insufficient development, overestimation of shear strength of concrete and insufficient amount of ties. To study failure mechanism of such piers, four 1/7 scaled cantilevered circular pier models were built and loaded. Four loading methods were used; 1) unilateral pushover loading, 2) unilateral cyclic loading, 3) bilateral cyclic loading and 4) unilateral hybrid loading. From the experimental results, it is known that piers suffered flexural shear failure under unilateral pushover and hybrid loadings while piers suffered compression shear failure under unilateral and bilateral cyclic loadings. It is also shown that the pier under bilateral loading suffered more significant damage than the pier under unilateral loading.

*Key Words: seismic design, bridge, seismic damage, loading test, shear, reinforced concrete column*

### 1. Introduction

Most extensive damage of bridges in the 1995 Kobe, Japan earthquake was the premature shear failure of reinforced concrete piers with termination of main reinforcements<sup>1)</sup>. Termination of main reinforcements with insufficient development length at several mid-heights as well as overestimated shear strength of concrete and insufficient ties resulted in the extensive damage. Shear strength of concrete was not critical in massive wall piers which were constructed at the early ages. However demand for reducing pier section to mitigate disturbance to river flow in river bridges and use of space of urban viaducts for city streets resulted in construction of slender piers in which shear strength was critical. However because significant earthquakes did not occur close to critical bridges in the last three decades, the risk of premature shear failure due to termination of main reinforcements was not recognized until recently.

The risk of premature shear failure was first recognized in 1978

Miyagi-ken-oki earthquake when several bridges suffered damage at their piers. It was well recognized in 1982 Urakawa-oki earthquake when Sizunai bridge suffered extensive damage at their piers<sup>2)</sup>. Design code was improved in 1980 by reducing the allowable shear stress of concrete and enhancing development of main bars (JRA 1980).

Various studies have been conducted for evaluation of seismic risk and retrofit of the premature shear failure. In 1987 effectiveness of steel jacketing to retrofit of bridge piers was first extensively studied based on a series of unilateral cyclic loading test which was conducted jointly by Public Works Research Institute and Metropolitan and Hanshin Expressway Public Corporations<sup>1) 3) 4)</sup>. Aims of the joint research were to develop an evaluation method on the vulnerability of premature shear failure and verify the effectiveness of steel jacket to circular hollow piers and rectangular solid piers. Based on the joint study, steel jacket was implemented to seismic retrofit of many bridges on Metropolitan and Hanshin Expressways. During the 1995 Kobe earthquake, several retrofitted

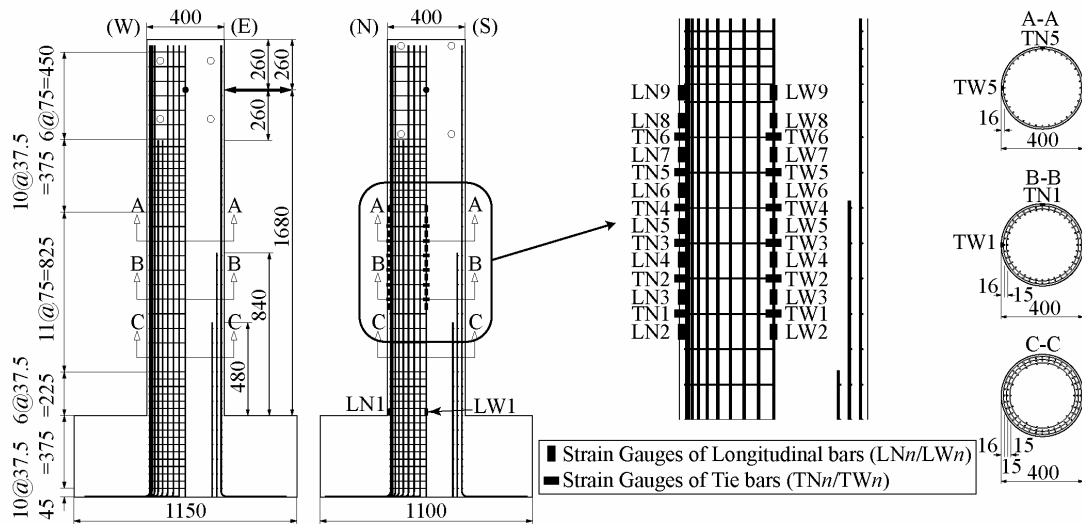


Fig. 1 Test Specimens

Table 1 Test Cases and Concrete Strength

Test Case	P	C-1	C-2	H
Loading Type	Unilateral Pushover	Unilateral Cyclic	Bilateral Cyclic	Unilateral Hybrid
Concrete Strength	29.6 MPa	26.6 MPa	29.6 MPa	29.8 MPa
Young's modules	25.8 GPa	26.7 GPa	25.8 GPa	36.1 GPa

Table 2 Longitudinal and Tie Reinforcements

Height (mm)	Longitudinal bar		Tie bar	
	Number	Areal Ratio	Interval	Volumetric Ratio
0 - 225	90	0.023	37.5 mm	0.0046
225 - 480	90	0.023	75.0 mm	0.0035
480 - 840	72	0.018	75.0 mm	0.0023
840 - 1050	36	0.009	75.0 mm	0.0011
1050 - 1680	36	0.009	37.5 mm	0.0022

piers did not suffer damage while un-retrofitted piers which were located very close to the retrofitted piers suffered extensive damage. This shows the effectiveness of seismic retrofit of piers. The evaluation and retrofit methods developed have been used as a standard retrofit method of bridge piers with termination of main reinforcements.

Based on a cyclic and hybrid loading test, failure mechanism of several piers of a viaduct which collapsed during the 1995 Kobe earthquake was clarified by Ikehata et al.<sup>5)</sup> Failure modes and levels depending on locations of termination of main bars and shear strength were clarified using 1/7 scaled models.

Because failure mechanism of premature shear failure still has many unsolved problems, and because it was typical damage in the 1995 Kobe earthquake, a large scale shake table test using E-Defense is planned based on NEES and E-Defense collaboration. A preliminary loading test was conducted at Tokyo Institute of Technology under funding of National Institute of Earth Science and Disaster Prevention. This paper presents the test results and preliminary analysis.

## 2. Specimens and Loadings

### 2.1 specimens

Four models as shown in Fig. 1 and Table 1 were constructed and loaded. The models have essentially the same property with the models used by Ikehata et al.<sup>5)</sup> The model piers are 1.68 m tall and have a circular section with a diameter of 400 mm. This is a 1/7 scaled model of a 11.7 m tall prototype pier with a diameter of 2.8 m. Shear span ratio is 4.2. Deformed bars with a diameter of 6 mm and 3 mm which were specially made for test<sup>5)</sup> was used for longitudinal and tie bars, respectively. The longitudinal reinforcements were set in 3 lines; 36 longitudinal bars for outer and center bars each and 18 longitudinal bars for the inner bars. Thus, 90 longitudinal bars were set in the column below 480 mm from the footing. Number of longitudinal bars was determined so that the longitudinal reinforcement ratio was 2.3 %. The inner and center bars were terminated at 480 mm and 840 mm, respectively, because they were terminated at 3,353 mm and 5,853 mm from the bottom in the prototype pier. Consequently, only outer bars were extended over 840 mm from the bottom of the pier. Section between the bottom

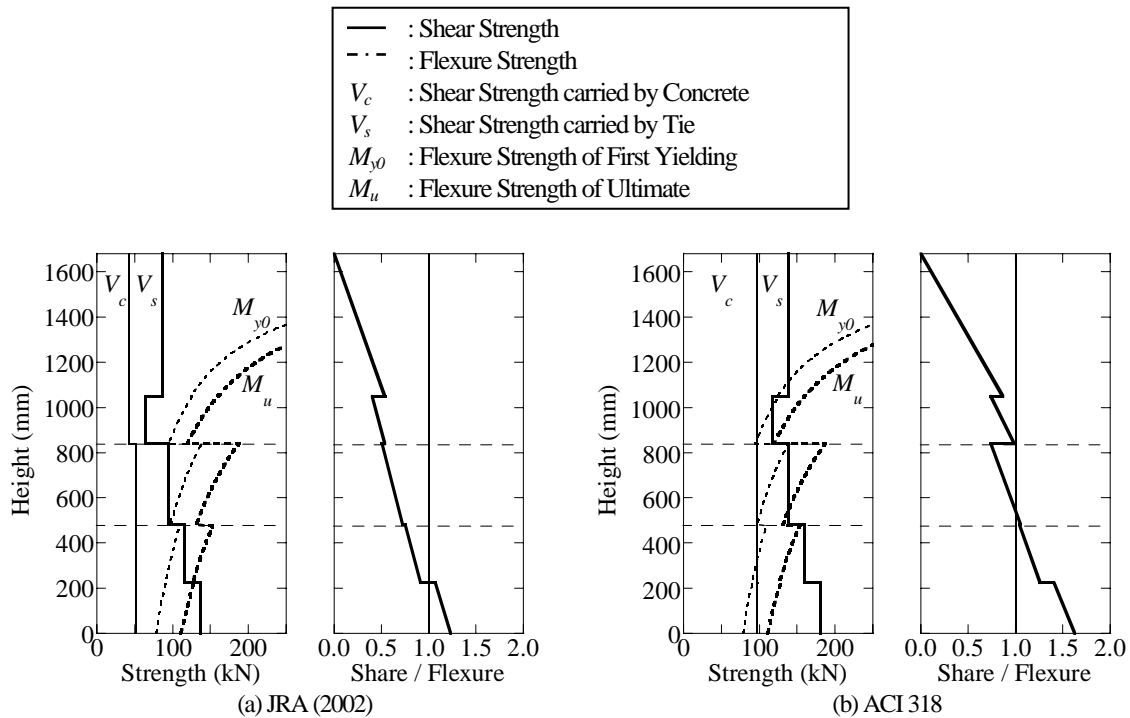


Fig. 2 Shear Strength and Flexure Strength of Model Piers

and 480 mm from the bottom, between 480 mm and 840 mm from the bottom and above 840 mm from the bottom is called hereinafter as sections A, B and C, respectively. Longitudinal reinforcement ratio at sections A, B and C was 0.9 %, 1.8 % and 2.3 %, respectively, as shown in Table 2.

Tie bars were provided to the outer, center and inner longitudinal bars. Tie bars were provided at every 75 mm at sections A and B. The same spacing was used for outer, center and inner tie bars. The volumetric tie reinforcement ratio was 0.11 % and 0.23 % at sections A and B, respectively, based on the design code<sup>6)</sup> as shown in Table 2. Tie spacing at section C was a half of the spacing at sections A and B based on the original design of prototype pier. The volumetric tie reinforcement ratio was 0.46 %. Amount of tie reinforcement was increased at the top of the pier (above 1,050 mm from the bottom) so that failure did not occur at this section.

Yield strength, tensile strength and elastic modulus of longitudinal reinforcements were 372.0 MPa, 498.6 MPa and 185.9 GPa, respectively, based on tensile test. Yield strain of longitudinal reinforcements was nearly 2000  $\mu$ . The same properties were assumed for tie bars.

Design concrete strength was 27 MPa. Normal Portland cement was used. Maximum size of aggregates was 13 mm. Concrete strength based on test was in the range of 26.6-29.8 MPa as shown in Table 1.

Fig. 2 compares the flexural and shear strengths of the models. Concrete strength of 29.6 MPa is assumed in this estimation. Because shear strength has inherently large scattering in its estimation, shear strengths evaluated by JRA<sup>6)</sup> and ACI 318<sup>7)</sup> are presented here. No safety factor was considered in the evaluation by

ACI 318. It is seen that JRA provides conservative estimation to the shear strength.

## 2.2 loadings

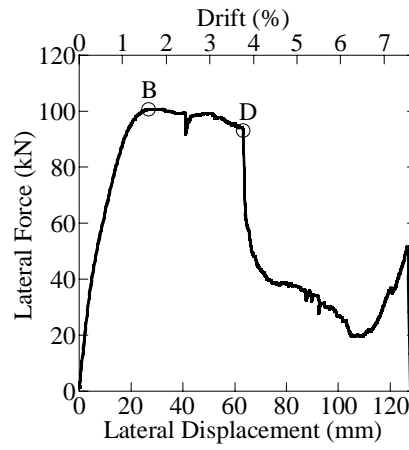
Four loading protocols were used in the test; 1) unilateral pushover loading, 2) unilateral cyclic loading, 3) bilateral cyclic loading and 4) unilateral hybrid loading. Since axial stress of prototype pier was 1.75 MPa, all loadings were conducted under a constant vertical load of 220 kN which resulted 1.75 MPa stress at the plastic hinge of piers. Lateral drift was used to regulate loading displacement. Since the first yield and the yield displacement<sup>6)</sup> are 5.4 mm and 7.6 mm, respectively, the yield displacement is equal to 0.45 % drift.

In the unilateral pushover loading, a pier model was loaded to failure under displacement control. Loading velocity was 1 mm/sec until 2.4 % drift. Because actuator control program had problem, the pier model was loaded by hand with loading velocity of about 0.5 mm/sec over this drift. In the unilateral cyclic loading, loading displacement was stepwisely increased from 0.5 % drift (=8.4 mm) to failure with an increment of 0.5 % drift. The pier was loaded three times at each loading displacement. In the bilateral cyclic loading, a circular orbit was used. The pier was first loaded in the W direction until the displacement reached 0.5 % drift. From this point, the pier was loaded three times along circular orbit. Finally, the pier was unloaded to the rest position from the W direction. This set of loadings was repeated until failure with an increment of 0.5 % drift.

In the hybrid loading, the EW component of ground acceleration measured at JR Takatori station during 1995 Kobe earthquake was



(a) Damage after Loading



(b) Lateral Force vs. Lateral Displacement Hysteresis

Fig. 3 Unilateral Pushover Loading

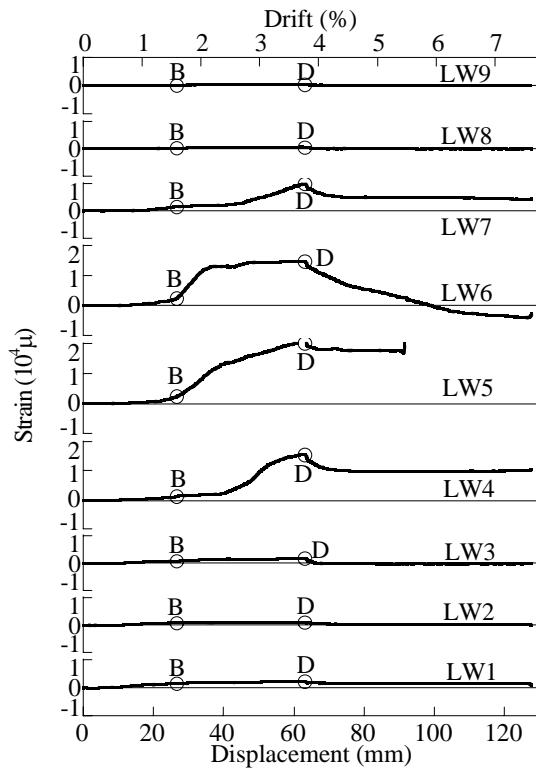


Fig. 4 Strains of a Longitudinal Bar at W surface under Unilateral Pushover Loading

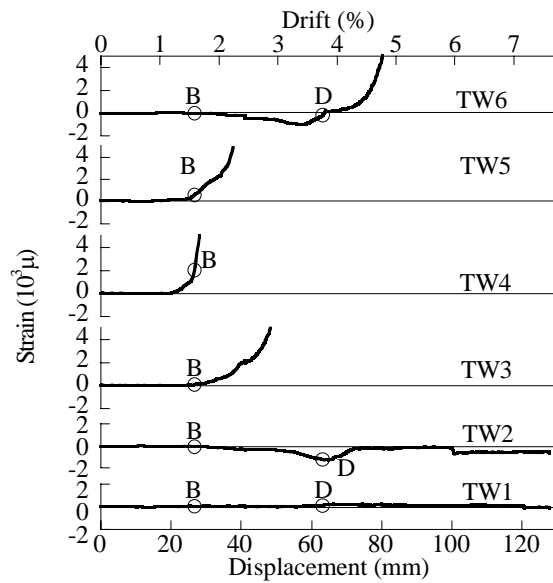


Fig. 5 Strains of Tie Bars Parallel to Loading (W surface) under Unilateral Pushover Loading

used. Intensity of the acceleration was reduced to 15 % (=1/7) of original record assuming that scale factor of mass and acceleration is 1/7. A numerical integration scheme which avoids displacement overshooting using a displacement reduction factor was employed in the hybrid loading<sup>8)</sup>. The P-Δ action of actuators was included in the numerical integration of equations of motion<sup>9)</sup>. Damping ratio of 2 % of critical was assumed. The time increment of numerical integration was 0.02 second.

In the above tests, vertical and lateral loading forces, vertical and lateral displacements at the loading points, and strains of longitudinal and tie bars were measured as shown in Fig. 1.

### 3. Failure Modes

#### 3.1 failure modes and performance under uniailateral pushover and cyclic loadings

Fig. 3 shows the failure mode after the loading and the lateral force vs. lateral displacement hysteresis of the pier under the uniailateral pushover loading. Flexural cracks were first developed in tension at 840 mm from the bottom (refer to Fig. 1) where center longitudinal bars were terminated (designated as upper termination

zone hereinafter), and they subsequently extended to the bottom of pier in compression. The lateral restoring force took a peak value of 100.8 kN at 1.6 % drift which is hereinafter designated as Point B. Subsequently the lateral restoring force slowly deteriorated to have a sharp deterioration at 3.8 % drift, which is designated hereinafter as Point D.

Fig. 4 shows strains at 9 heights of an outer longitudinal bar which is located at middle of the compression and tension fibers (LW1-LW9, refer to Fig. 1). It is noted that the longitudinal bar slightly yielded at the plastic hinge (LW1) at Point B, but only limited increase of strain occurred. Strains of the longitudinal bar at LW4-LW6 (712.5-862.5 mm from the bottom) started to sharply increase at Point B, and they exceeded 10,000  $\mu$  at Point D. It should be reminded here that center longitudinal bars were terminated at 840 mm from the bottom of pier (between LW5 and LW6). This resulted in strains over 10,000  $\mu$  in the outer longitudinal bars at LW4-LW6.

Fig. 5 shows strains of ties for outer longitudinal bars parallel to the loading direction (TW1-TW6, refer to Fig. 1). It should be reminded here that center longitudinal bars were terminated at the height where TW4 was measured. It is noted that strain at TW4 started to sharply increase slightly before reaching Point B and yielded subsequently. This will be described later. Tie bars at TW5 and TW3 yielded before reaching Point D, however tie bar at TW6 (975 mm from the bottom) yielded after Point D. This shows that new extension of shear cracks occurred at TW6 after Point D.

On the other hand, Fig. 6 shows damage of pier after the unilateral cyclic loading. Flexural cracks were first initiated at the upper termination zone, and they turned into diagonal cracks. They extended subsequently directing to the bottom of pier at 2.0 % drift. But diagonal cracks did not progress furthermore, and separation of the covering concrete and buckling of longitudinal bars progressed at the upper termination zone where flexural cracks were first initiated at 2.5 % drift. Consequently, compression shear failure occurred at the termination zone. The lateral restoring force reached its peak value of 103.4 kN at 1.5 % drift. This lateral force remained until 2.0 % drift with a sudden deterioration at 2.5 % drift.

Fig. 7 shows strains of an outer longitudinal bar in the tension and compression fibers (LW1-LW9, refer to Fig. 1). Because measurement of bar strains under cyclic loading is extremely difficult, only reliable strains have to be carefully evaluated. It is seen that longitudinal bars first yielded at 0.5 % drift at LW1 (17.25 mm from the bottom of the pier). Strain at LW6 (22.5 mm above the termination of center longitudinal bars) sharply increased to nearly 0.01 following LW1 at 1.0 % drift, however it further increased over 0.02 at 1.5 % drift. Strain at LW1 did not increase as sharply as LW6 at 1.5 % drift. It apparently shows that flexural damage first progressed until 0.5 % drift, however shear failure subsequently became predominant after 1.0 % drift.

Fig. 8 shows strains of tie bars which are parallel to the loading direction. Strains of tie bars were limited until diagonal cracks occurred at 1.5 % drift. However, over 1.5 % drift tie strain sharply

increased at TN4 (same height with termination of center longitudinal bars), which resisted shear after diagonal cracks were initiated.

It is noted that both the flexural shear failure and the compression shear failure presented above occurred during the 1995 Kobe earthquake. Under unilateral pushover loading, diagonal shear cracks initiated at the upper termination zone extended along the shear cracks. In reality, unilateral pushover loading does not exist during an earthquake. However if a long pulse ground acceleration which is likely included in near-field ground motions is predominant to result in oscillation of a bridge in one direction, the pier may fail in flexural shear. On the other hand, the compression failure is developed at the upper termination under cyclic loading. Because flexural and shear strengths deteriorate at this zone once compression failure occurs, further extension of diagonal cracks does not occur. Consequently, a pier is likely to fail in compression shear if it is subjected to repeated loading in both directions.

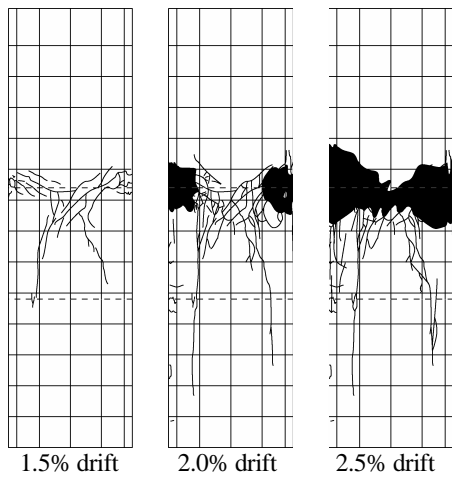
It is noted that the column specimens in this study had shear and flexural capacities which are virtually the same level at the upper termination as shown in Fig. 2(b). This could result in the predominated effect of loading protocol on the failure mechanism. It is interest to further study whether similar level of loading protocol dependence on the failure mechanism is developed for columns with other ratios of shear and flexural capacities.

### 3.2 effect of bilateral loadings

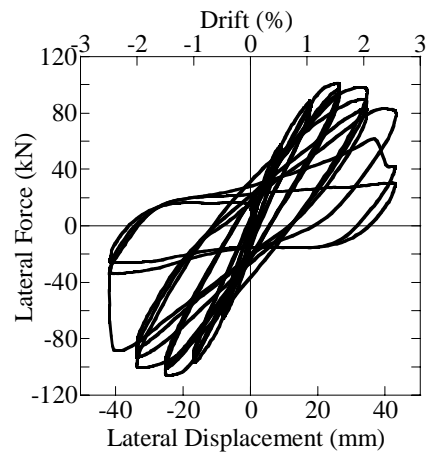
Fig. 9 shows failure after loading and the lateral force vs. lateral displacement hysteresis of the pier under the bilateral cyclic loading. Flexural cracks occurred at the upper termination zone, and the pier failed in compression shear. Failure of core concrete as well as flexural cracks were more extensive under the bilateral cyclic loading than the unilateral cyclic loading, however diagonal shear cracks were slightly less under the bilateral cyclic loading than the unilateral cyclic loading. General trend of the lateral force vs. lateral displacement hysteresis under the bilateral cyclic loading is similar to that under the unilateral cyclic loading. However the peak restoring force under the bilateral excitation is nearly 10 % less than that under the unilateral loading.

Figs. 10 and 11 show strains of longitudinal bars at W and N surfaces. In the longitudinal bars at both surfaces strains at the plastic hinge zone (LW1 and LN1) are more dominant than strains at other locations at 0.5 % drift. However, strains at the termination of center longitudinal bars (LW6 and LN6) sharply increased to have the similar values with LW1 and LN1 at 1.0 % drift, and they further progressed over LW1 and LN1 at 1.5 % drift.

Figs. 12 and 13 show strains of tie bars at N and W surfaces. Strains of tie bars located at the height of termination of center longitudinal bars (TW4 and TN4) and 75 mm above this height (TW5 and TN5) are larger than strains at other heights. Strains at TW4, TN4, TW5 and TN5 started to increase at 1.5 % drift, and they sharply progressed to nearly yield strain and over 0.02 at 1.5 %



(a) Progress of Damage after Loadings



(b) Lateral Force vs. Lateral Displacement

Fig. 6 Unilateral Cyclic Loading

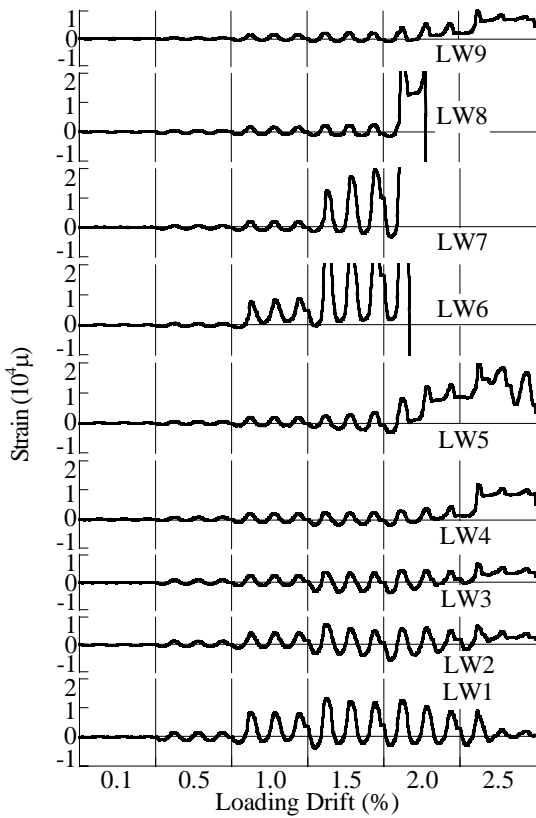


Fig. 7 Strains of a Longitudinal Bar at W surface under Unilateral Cyclic Loading

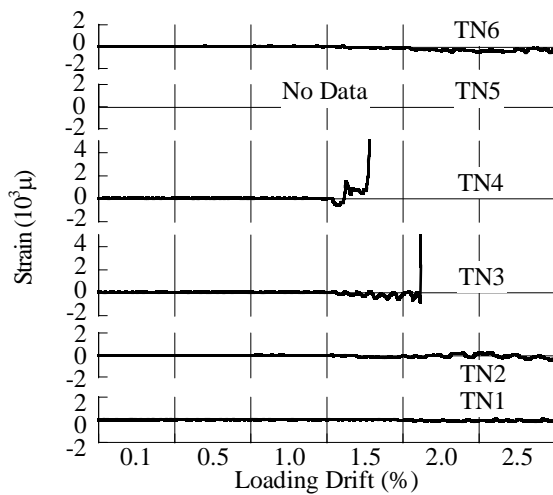
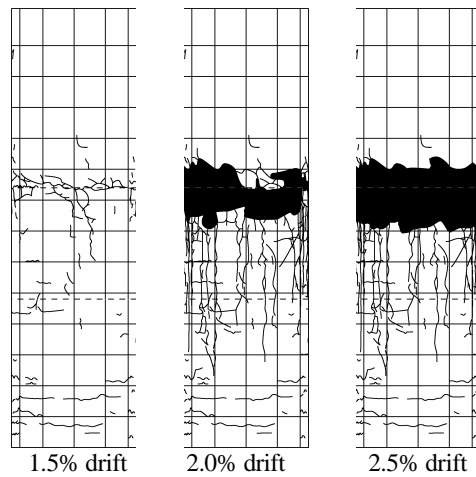
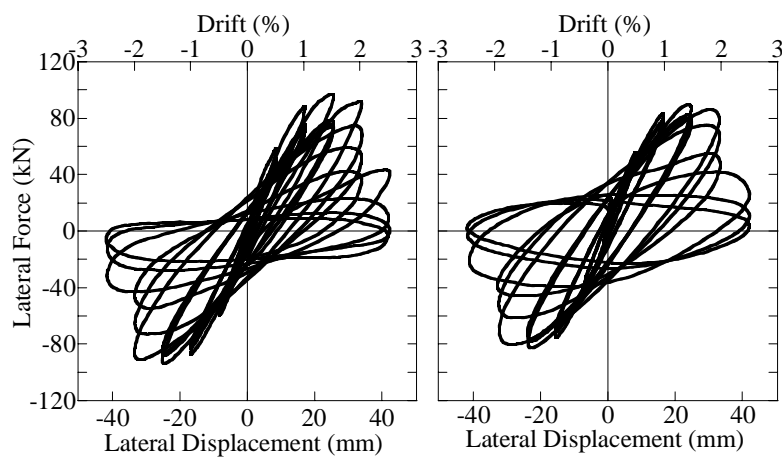


Fig. 8 Strains of Tie Bars Parallel to Loading (N surface) under Unilateral Cyclic Loading



(a) Progress of Damage after Loadings



(b) Lateral Force vs. Lateral Displacement Hysteresis: EW direction (left) and NS direction (right)

Fig. 9 Bilateral Cyclic Loading

drift and 2.0 % drift, respectively.

### 3.3 performance under unilateral hybrid loading

Fig. 14 shows response displacement of the pier as well as the imposed ground acceleration under the unilateral hybrid loading. Since the pier failed in shear at 4.7 s loading was terminated. The peak displacement at the loading point is 26.0 mm at 1.9 s and -48.9 mm at 2.5 s.

Fig. 15 shows failure mode of the column after loading. A large diagonal crack extended from the upper termination zone to 300 mm from the bottom. This is similar to the flexural shear failure mode which was developed under unilateral pushover loading except several diagonal cracks which were developed in the alternative direction.

Fig. 16 shows the lateral force vs. lateral displacement hysteresis of the pier. The peak restoring force at 1.6 % drift is 107.2 kN, which is close to the peak restoring force developed under the pushover loading.

Fig. 17 shows strains of longitudinal bars at the W surface

located perpendicular to the loading direction. Strain of longitudinal bar at 22.5 mm above the upper termination (LW6) started to sharply increase at 2.3 s followed by LW7-LW9. Fig. 18 shows strains of tie bars. Strains of ties were limited until the pier response first reached 1.5 % drift, but strains at TW4 and TW5 started to sharply increase over this point.

### 4. Shear Strength Carried by Concrete and Ties

The shear strength of the reinforced concrete columns is assumed here to be derived from two contributions as

$$V = V_c + V_s \quad (1)$$

in which  $V_c$  and  $V_s$  are the shear force carried by concrete and ties, respectively. The shear force carried by concrete is composed of the shear force due to aggregate interlocking along the cracks, the shear force of the concrete at compression zone and the shear force due to the dowel action of the longitudinal reinforcements in tension. Because theoretical estimation of aggregate interlocking and shear force of the concrete in compression is difficult, the shear force carried by concrete is evaluated based on test results.  $V_s$  is

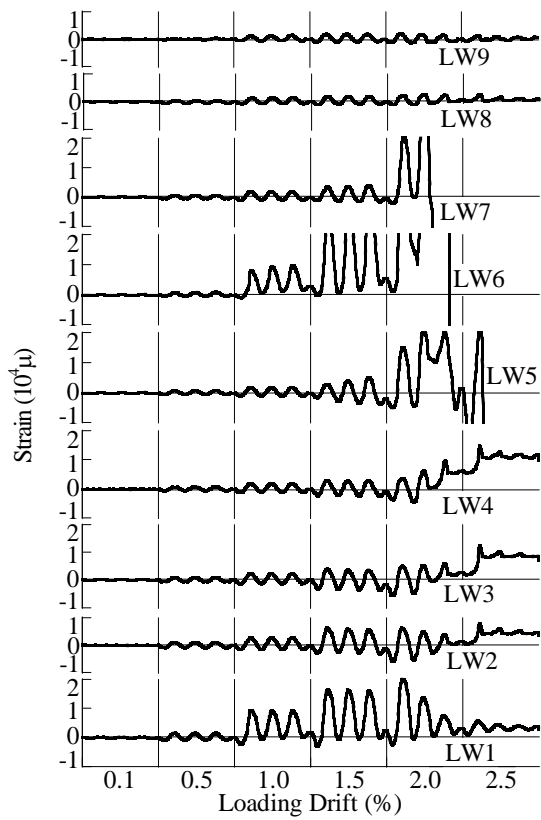


Fig. 10 Strains of a Longitudinal Bar at W surface under Bilateral Cyclic Loading

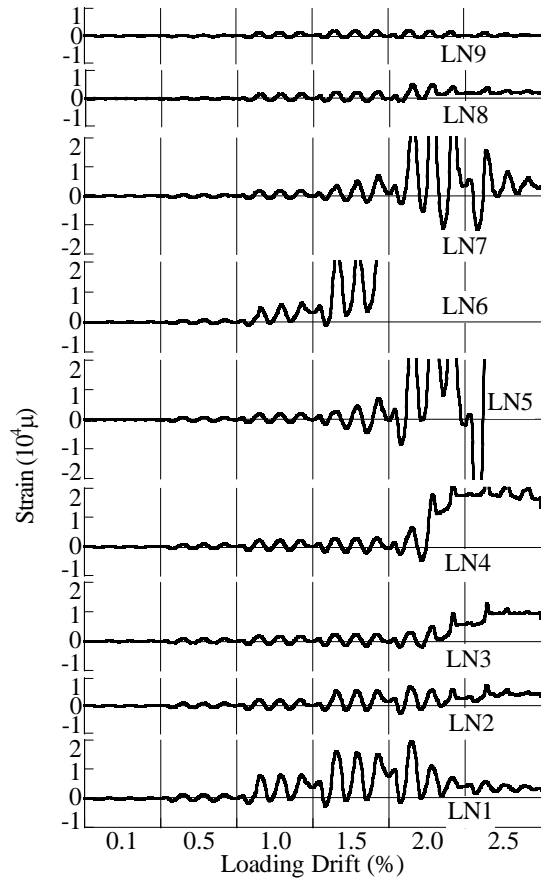


Fig. 11 Strains of a Longitudinal Bar at N face under Bilateral Cyclic Loading

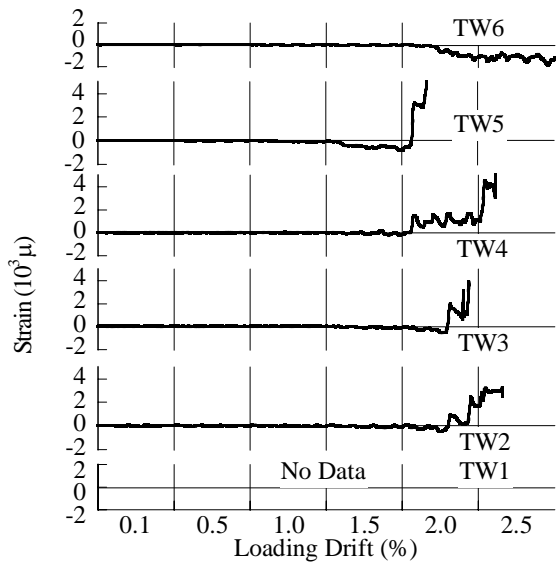


Fig. 12 Strains of Tie Bars at W face under Bilateral Cyclic Loading

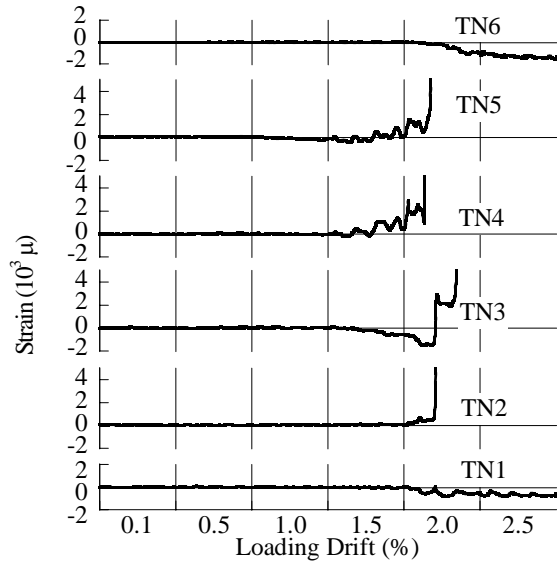


Fig. 13 Strains of Tie Bars at N face under Bilateral Cyclic Loading

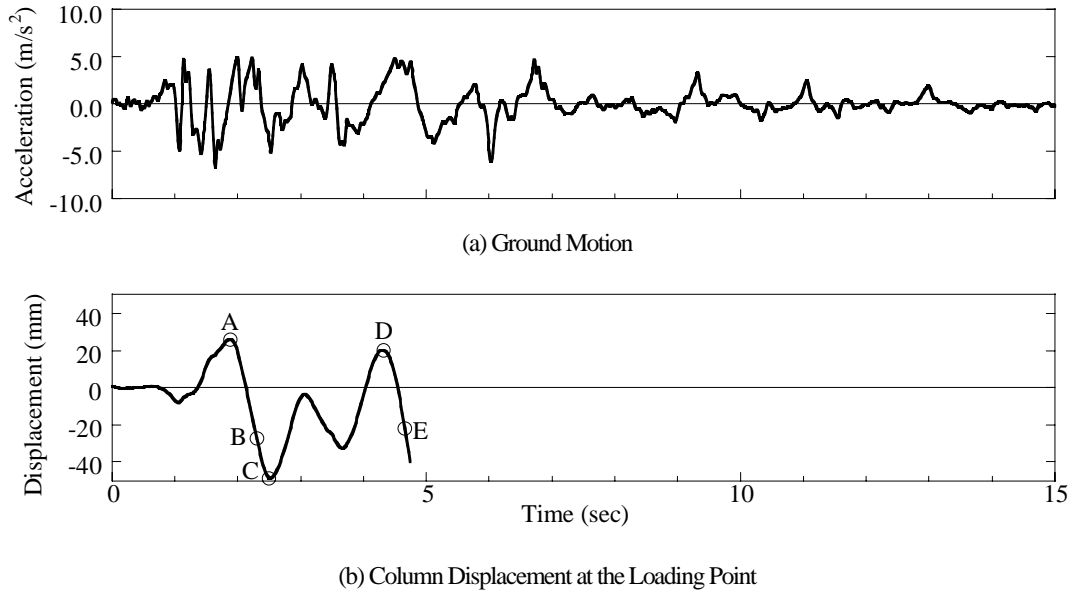


Fig. 14 Response of the Model Column under Hybrid Loading

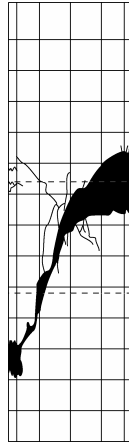


Fig. 15 Damage after Loading

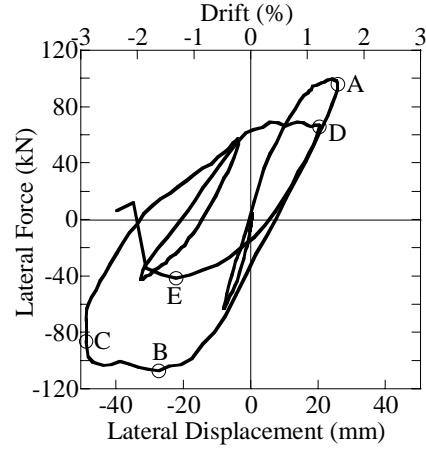


Fig. 16 Lateral Force vs. Lateral Displacement Hysteresis

approximated by the traditional truss analogy theory as

$$V_s = \sum_{i=1}^n 2A_{ti} E_t \varepsilon_{ti} \sin \beta_i \quad (2)$$

where  $n$  = number of the effective ties,  $A_{ti}$  = area of  $i$ -th tie,  $E_t$  = elastic modulus of ties;  $\varepsilon_{ti}$  = strain of  $i$ -th tie at each lateral displacement; and  $\beta_i$  = angle from tie force to lateral force. The shear force carried by concrete was evaluated for the pier subjected to unilateral pushover loading by Eq. (1) based on measured tie strains. For this purpose, the shear force carried by ties was evaluated at four points (Points A, B, C and D) as shown in Fig. 19; Points B and D were already defined. Point A represents the instance of suffering first diagonal cracks, and Point C represents the instance when full cracks occurred.

As shown in Fig. 20, strain at TW4 (refer to Fig. 1) is small until Point A. Assuming that any ties did not resist shear at this stage, the shear force carried by concrete at Point A,  $V_{C,A}$ , can be evaluated

by the measured shear force of the pier at Point A,  $V_{,A}$ , as

$$V_{C,A} = V_{,A} \quad (3)$$

After the initial cracks, the tie strain significantly increased and exceeded yielding level at Point B as shown in Fig. 20. The cracks occurred between 630 mm and 950 mm, and there were seven effective ties within this range, as shown in Fig. 21(a). By substituting  $E_t \varepsilon_{ti}$  in Eq. (2) by yield stress of tie,  $\sigma_{ty}$ , and assuming  $i=7$ , the shear force carried by concrete at Point B,  $V_{C,B}$ , may be obtained by the measured shear force of the pier at Point A,  $V_{,B}$ , as

$$V_{C,B} = V_{,B} - V_{S,B} \quad (4)$$

At the occurrence of full crack (Point C), there are twenty effective ties, as shown in Fig. 21(b). Therefore assuming the yield of twenty ties, the shear force carried by concrete at Point C,  $V_{C,C}$ , may be obtained from the measured shear force of the pier at Point C,  $V_{,C}$ , as

$$V_{C,C} = V_{,C} - V_{S,C} \quad (5)$$

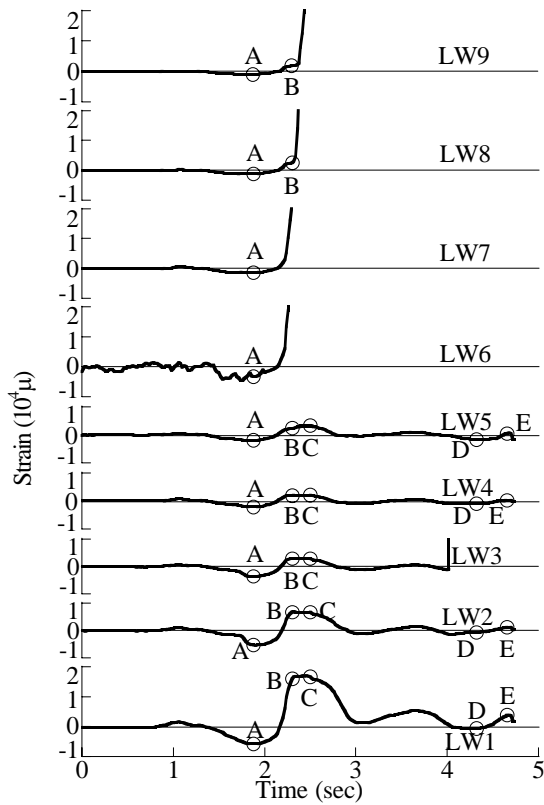


Fig. 17 Strains of a Longitudinal Bar at W surface under Unilateral Hybrid Loading

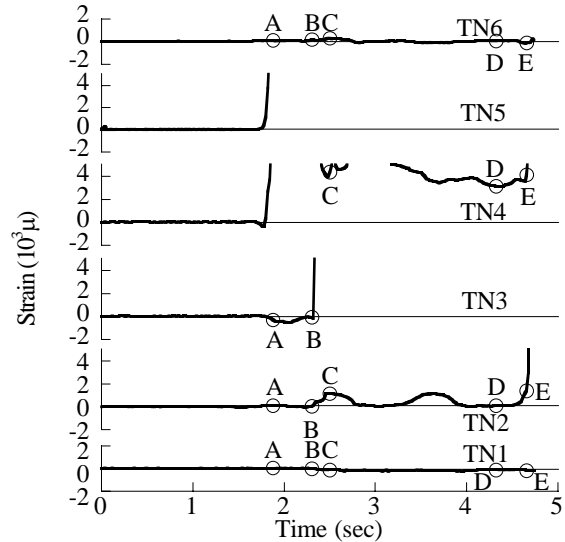


Fig. 18 Strains of Tie Bars Parallel to Loading (N surface) under Unilateral Hybrid Loading

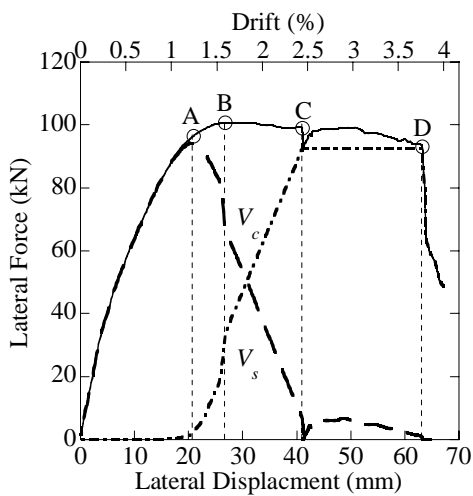


Fig. 19 Shear Force carried by Concrete and Ties

The shear force carried by ties increases as number of effective ties increases between Points B and C. Consequently, the shear force carried by ties between Points B and C are evaluated by assuming that it linearly increases as the lateral displacement increases from Point B to Point C.

After the occurrence of full cracks, the shear force carried by ties remained constant and the shear force of the concrete deteriorated slightly as the crack widths increased. The shear force carried by concrete starts to deteriorate significantly at Point D as a result of opening of the cracks.

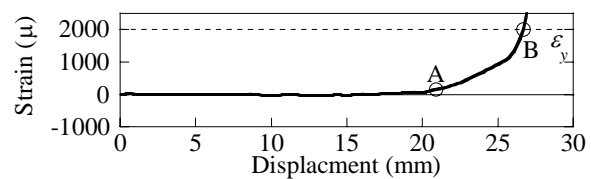
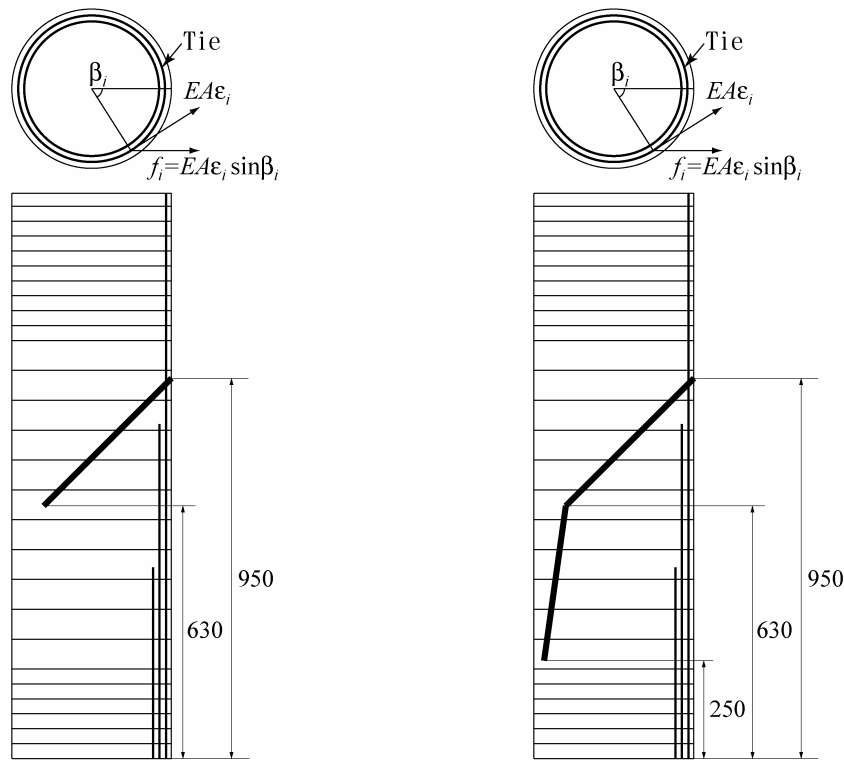


Fig. 20 Strain of Tie at TW4 (825 mm from the bottom)

Based on the above assumptions, the shear force carried by ties and concrete was estimated as shown in Fig. 19. The shear stress was then obtained by dividing the shear force by area of the core concrete as shown in Fig. 22. It is noted that shear stress should be evaluated by dividing shear force by 80 % the column sectional area in ACI 318<sup>7)</sup> and Priestley et al. method<sup>10)11)</sup>, it was assumed here that the 80 % the column section area corresponded to the area of core concrete. Shear stresses by JRA<sup>6)</sup>, ACI 318<sup>7)</sup> and Priestley et al.<sup>10)11)</sup> are presented here for comparison. It is seen that the shear stress evaluated from the test is less than 1 MPa at 1.2 % drift and it



(a) At the Maximum Lateral Force (Point B)

(b) At the Occurrence of the Full Crack (Point C)

Fig. 21 Number of Effective Ties which Resist Shear under Unilateral Pushover Loading

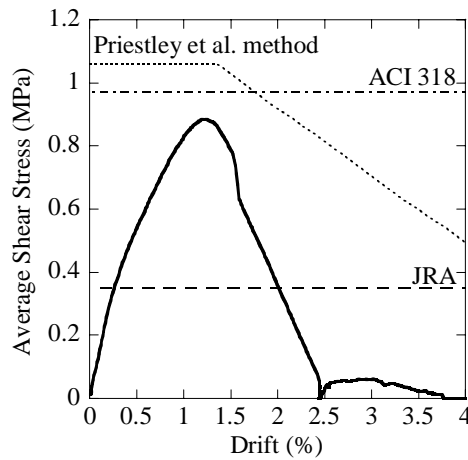


Fig. 22 Shear Stress carried by Concrete

deteriorated as loading displacement increased after the longitudinal bars yielded. It is noted that JRA and ACI 318 represent shear strength of concrete beam subjected to pushover loading. Consequently there must be discrepancy between shear carried by concrete which was estimated based on this experiment and estimated shear capacity by JRA and ACI 318.

## 5. Conclusions

Loading experiment was conducted on four 1/7 scaled model piers using four loading protocols to clarify the failure mechanism of piers with terminations of main reinforcements with insufficient

development length. The following conclusions may be deduced from the results presented herein;

- Flexural shear failure occurred under the unilateral pushover loading, while compression shear failure occurred under the unilateral cyclic loading. Failure modes depend on loading paths. Both failure modes occurred during the 1995 Kobe earthquake.
- Dependence of loading protocols on the failure mechanism is of interest for column with other flexural and shear capacity ratios. Further study is required to clarify this point.
- Dependence of shear stress carried by concrete on progress of failure was evaluated as shown in Fig. 22 under the unilateral

pushover loading.

- Flexural cracks and damage of core concrete are more extensive under bilateral cyclic loading than unilateral cyclic loading. On the other hand, because diagonal shear cracks distribute at various directions, significant diagonal cracks which are developed along diagonal failure planes under unilateral cyclic loading do not take place under bilateral cyclic loading.
- Flexural shear failure occurred under the unilateral hybrid loading using JR Takatori station ground motion measured during the 1995 Kobe earthquake. Failure mode under the unilateral hybrid loading is very similar to that under the unilateral cyclic loading.

### Acknowledgements

The authors appreciate invaluable guidance of Dr. Shoji Ikeda, Professor Emeritus, Yokohama National University on the failure mechanism of the prototype bridge and loading test method. This research was conducted based on the funding of the National Institute of Earth Science and Disaster Prevention in conjunction with the large scale bridge shake table experiment project based on NEES and E-Defense collaboration.

### References

- 1) Kawashima, K. and Unjoh, S., The Damage of Highway Bridges in the 1995 Hyogo-ken Nanbu Earthquake and Its Impact on Japanese Seismic Design, *Journal of Earthquake Engineering*, Vol. 1, No. 3, pp. 505-541, 1997.
- 2) Asanuma, H., Damage of Sizunai Bridge, *Journal of Civil Engineering*, Vol. 25, No. 11, pp. 15-20, 1983 (in Japanese).
- 3) Akimoto, T., Nakajima, H., and Kogure, F., Seismic Strengthening of Reinforced Concrete Piers on Metropolitan Expressway, *Proc. First US-Japan Workshop on Seismic Retrofit of Bridges*, pp. 258-298, Public Works Research Institute, Tsukuba, Japan, 1990.
- 4) Matsuura, Y., Nakamura, I. and Sekimoto, H., Seismic Strengthening for Reinforced Concrete Bridge Piers of Hanshin Expressway, *Proc. First US-Japan Workshop on Seismic Retrofit of Bridges*, pp. 299-317, Public Works Research Institute, Tsukuba, Japan, 1990.
- 5) Ikehata, S., Adachi, K., Yamaguchi, T. and Ikeda, N., Seismic Performance of RC Bridge Piers based on Quasi-static Dynamic Loading Tests, *Proc. JCI*, Vol. 23, No. 3, pp. 1255-1260, 2001 (in Japanese).
- 6) Japan Road Association, *Part V Seismic Design-Design Specifications of Highway Bridges*, Maruzen, Tokyo, Japan, 2002.
- 7) ACI Committee 318, *Building Code Requirements for Structural Concrete (ACI 318-95) and Commentary (318R-95)*, American Concrete Institute, Farmington Hills, USA, 1995.
- 8) Shing, P. B., Vannan, M.T. and Cater, E., Implicit Time Integration for Pseudodynamic Tests, *Earthquake Engineering and Structural Dynamics*, Vol. 20, pp. 551-576, 1991.
- 9) Nagata, S., Kawashima, K. and Watanabe, G., Effect of P- $\Delta$  Action of Actuators in a Hybrid Loading Test, *Proc. 13th World Conference on Earthquake Engineering*, Paper No. 881, Vancouver, Canada, 2004.
- 10) Priestley, N.M.J., Seible, F. and Calvi, M., *Seismic Design and Retrofit of Bridges*, John Wiley & Sons, New York, USA, 1996.
- 11) Kowalsky, M. J. and Priestly, M. J. N., Improved Analytical Model for Shear Strength of Circular Reinforced Concrete Columns in Seismic Regions, *ACI Structural Journal*, Vol. 97, No. 3, 2000.

(Received September 11, 2006)